Available online at www.sciencedirect.com
ScienceDirect
Journal of Sound and Vibration 324 (2009) 1086–1110
JOURNAL OF SOUND AND VIBRATION
www.elsevier.com/locate/jsvi

Numerical analysis of acoustic modes using the linear least squares method of fundamental solutions

C.C. Tsai[1], D.L. Young*, C.L. Chiu, C.M. Fan[2]

Department of Civil Engineering & Hydrotech Research Institute, National Taiwan University, Taipei 10617, Taiwan

Received 8 May 2008; received in revised form 13 May 2008; accepted 22 February 2009
Handling Editor: L.G. Tham
Available online 26 March 2009

Abstract

The method of fundamental solutions (MFS) has been proved to be an accurate and efficient meshless numerical method to solve acoustic eigenproblems. Traditionally, the technique of the singular value decomposition (SVD) is employed to obtain the corresponding contours of acoustical modes after the eigenvalues are solved. However, it is found that the mode shapes are sensitive to the source locations of the MFS. In this paper, we try to derive a robust meshless numerical scheme to obtain the contours of acoustical modes based on the linear least squares method of fundamental solutions (LSMFS) by specifying an additional normalized dual boundary condition. The failure for determining the mode shapes by specifying a normalized data at boundary locations near or on the nodes are examined. Moreover, it is demonstrated that the mode shapes of degenerate eigenmodes can be distinguished by specifying the boundary data at different boundary points. Furthermore, a normalization procedure is introduced for degenerate eigenmodes. Three numerical experiments with regular and irregular boundaries are carried out to validate the proposed method. Mode shapes obtained by the linear LSMFS are in good agreement with the analytical solutions and also the results obtained by the finite element method. In addition, the robustness and accuracy of the eigenvalues obtained with respect to different locations of source points by the linear LSMFS in conjunction with direct determinant search method are also revisited.

1. Introduction

In the last decade, researchers have paid attention to the meshless numerical methods without employing the concept of element. The initial idea of meshless methods dated back to the smoothed particle hydrodynamics (SPH) method for modeling astrophysical phenomena [1]. The method of fundamental solutions (MFS) is another important category of the meshless numerical methods which approximates the solutions by a linear superposition of the fundamental solutions with sources located outside the

*Corresponding author. Tel./fax: +886 2 2362 6114.
E-mail address: dlyoung@ntu.edu.tw (D.L. Young).
[1]Now at Department of Information Technology, Toko University, Chia-Yi County 61363, Taiwan.
[2]Now at Department of Harbor and River Engineering, National Taiwan Ocean University, Keelung 20224, Taiwan.

0022-460X/$ - see front matter © 2009 Elsevier Ltd. All rights reserved.
doi:10.1016/j.jsv.2009.02.032

computational domain to avoid the singularity [2–11]. Comparing to conventional numerical methods, such as the boundary element method (BEM) and the finite element method (FEM), the MFS is a meshless, integral-free and non-singular numerical method. The MFS was first proposed by Kupradze and Aleksidze in 1964 [2]. Later Mathon and Johnston [3] and Bogomolny [4] provided mathematical fundamentals for the MFS. Then the MFS was successfully applied to the potential flow problems [5], the biharmonic equation [6], the Poisson equation [7], the Stokes flow problems [8,9], and the diffusion equations [10,11]. In this paper, we will concentrate on the MFS for acoustic problems, which are governed by the Helmholtz equation. The detailed descriptions and comparisons of MFS with other numerical methods can be found in Refs. [8,12–15].

Kondapalli et al. [16] were among the first to apply the MFS for the Helmholtz equation in the analysis of acoustic scattering in fluids and solids. On the other hand, Karageorghis [17] applied the MFS to obtain eigenvalues of the Helmholtz equation in 2D simply-connected domains, and Chen et al. [18] solved eigenvalues in 2D multiply-connected domains. Tsai et al. [19] recently summarized the MFS applications for eigenvalues in 2D and 3D domains with and without interior holes. Recently Reutskiy [20] proposed a new algorithm to determine the eigenvalues in the MFS which is totally different from the singular value decomposition (SVD) technique and direct determinant search method. The capability of determination of the eigenvalues by the MFS is unquestionable. Alves and Valtchev [21] compared the MFS with the plane waves method and concluded that the plane waves method can be seen as an asymptotic case of the MFS. Instead of using fundamental solution in the MFS, the non-dimensional dynamic influence function method proposed by Kang et al. [22–24] adopted only the imaginary part of the fundamental solution. Although adoption of the imaginary part of the fundamental solution can form a boundary-type and singularity-free method, the non-dimensional dynamic influence function method can be treated as a special case of the imaginary-part dual BEM [25].

In those previous mentioned works [17–19], the MFS in conjunction with the direct determinant search method was applied to obtain the eigenvalues. Furthermore, it was found that the eigenvalues obtained by the MFS are highly accurate with very few nodes and insensitive to the locations of sources. However, the MFS has not yet been applied to obtain the mode shapes of acoustical eigenmodes to the best knowledge of the authors.

The SVD has been maturely applied to obtain the contours of acoustical modes after the eigenvalues are solved by applying the boundary integral equation method (BIEM) [26,27]. However, it is found that the ill-conditionings of the MFS [28] and the singularities of eigenmodes interacted and made the mode shapes sensitive with respect to the locations of source points when the MFS associated with SVD was utilized. On the other hand, Chen et al. [29] applied the dual BEM to obtain the mode shapes of a square cavity by specifying an additional normalized dual boundary condition. It results in an over determined system of linear equations with proper conditioning when the prescribed idea is applied to the MFS and thus the linear least squares method of fundamental solutions (LSMFS) [30] must be applied. Furthermore, it is demonstrated in our numerical experiments that the degenerate modes can be distinguished by specifying the boundary data at different boundary points. Besides, the phenomena are examined when the normalized data at boundary locations near or on the nodes. For degenerate eigenmodes, a normalization procedure which is also based on the linear LSMFS is derived. Three numerical experiments with and without degenerate acoustic modes for simple and complex geometries are carried out, in which both Dirichlet and Neumann boundary conditions are considered. In the following sections, we will address consequently the linear LSMFS, numerical results and conclusions.

2. Linear LSMFS

For acoustical problems, the governing equation is the Helmholtz equation with boundary conditions:

$$\begin{cases} (\nabla^2 + k^2)u(\mathbf{x}) = 0, & \mathbf{x} \in \Omega \\ u(\mathbf{x}) = 0, & \mathbf{x} \in \Gamma^D \\ \dfrac{\partial u(\mathbf{x})}{\partial n} = 0, & \mathbf{x} \in \Gamma^N \end{cases} \tag{1}$$

where $\mathbf{x}$ are the spatial coordinates, ∇^2 is the Laplacian, k is the wavenumber, Ω is the domain of interest, $\Gamma = \Gamma^D + \Gamma^N$ is the boundary of Ω and $\partial/\partial n$ is the directional derivative with respect to the outward normal vector $\vec{n}$ (Fig. 1(a)). The fundamental solution of the Helmholtz equation, Eq. (1), is defined by

$$-(\nabla^2 + k^2)G_k(\mathbf{x}, \mathbf{s}) = \delta(\mathbf{x}, \mathbf{s}) \tag{2}$$

where $\mathbf{s}$ are the coordinates of source points. Then, the 2D fundamental solution can be obtained [17–19]:

$$G_k(\mathbf{x}, \mathbf{s}) = \frac{-i}{4} H_0^{(2)}(k|\mathbf{x} - \mathbf{s}|) \tag{3}$$

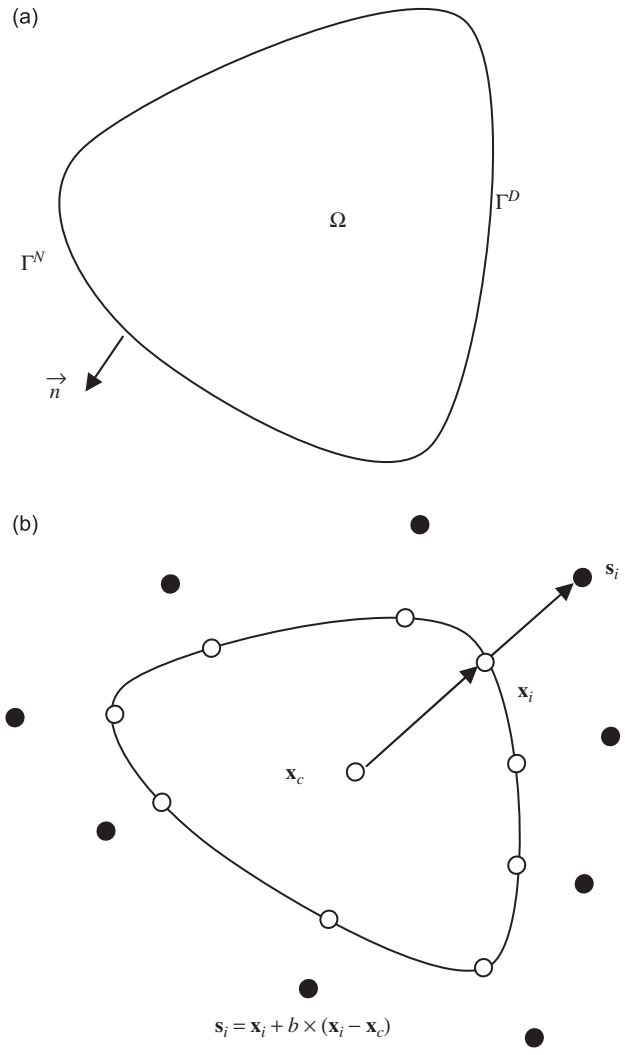

Fig. 1. Schematic diagram of the distribution of the source and boundary field points.

Table 1
The four lowest eigenvalues for different nodes (Example 1, $b = 0.8$).

	Analytic solution	$N = 36$	$N = 42$	$N = 48$	$N = 54$	$N = 60$
Mode 1	3.7241918	3.724197	3.724192	3.724192	3.724192	3.724192
Mode 2	5.0862171	5.086209	5.086217	5.086217	5.086217	5.086217
Mode 3	6.5938166	6.593820	6.593817	6.593817	6.593817	6.593817
Mode 4	6.7727103	6.772700	6.772710	6.772710	6.772710	6.772710

Table 2
The four lowest eigenvalues for different locations of source points (Example 1, $N = 54$).

	Analytic solution	$b = 0.00001$	$b = 0.2$	$b = 0.5$	$b = 0.8$	$b = 2.0$
Mode 1	3.7241918	3.724250	3.724190	3.724192	3.724192	3.724192
Mode 2	5.0862171	5.086230	5.086219	5.086217	5.086217	5.086217
Mode 3	6.5938166	6.593800	6.593819	6.593817	6.593817	6.593817
Mode 4	6.7727103	6.772700	6.772706	6.772710	6.772710	6.772710

Table 3
The four lowest eigenvalues for different nodes (Example 1, by FEM).

	Analytic solution	$N = 800$	$N = 1800$	$N = 3200$	$N = 5000$	$N = 7200$
Mode 1	3.724192	3.73076	3.72711	3.72583	3.72524	3.72492
Mode 2	5.086217	5.10188	5.09318	5.09014	5.08873	5.08796
Mode 3	6.593817	6.62669	6.60842	6.60203	6.59907	6.59747
Mode 4	6.772710	6.80402	6.78666	6.78057	6.77774	6.77620

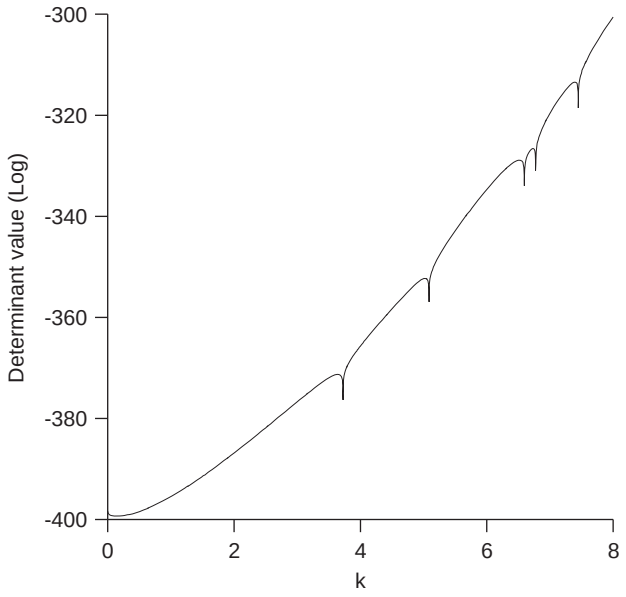

Fig. 2. The result of the direct determinant search method (Example 1).

where $H_0^{(2)}()$ is the Hankel function of the second kind of order zero. For simplicity, we define the following notations:

$$\begin{cases} U_k(\mathbf{x},\mathbf{s}) = G_k(\mathbf{x},\mathbf{s}) \\ L_k(\mathbf{x},\mathbf{s}) = \dfrac{\partial G_k(\mathbf{x},\mathbf{s})}{\partial n_x} \end{cases} \tag{4}$$

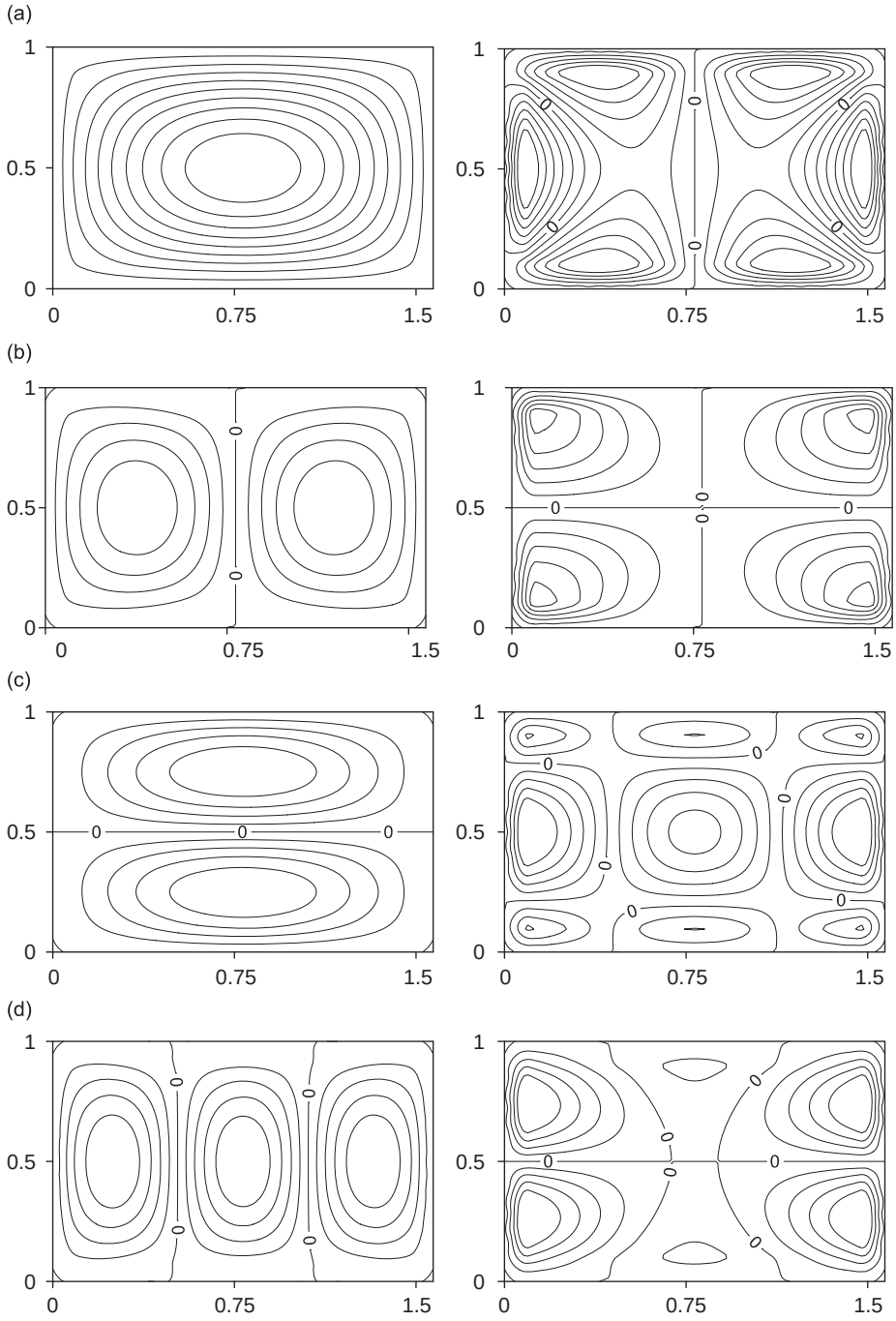

Fig. 3. The sensitivity of the mode shapes obtained by the SVD. (a) mode 1; (b) mode 2; (c) mode 3; (d) mode 4 (Example 1, $N = 52$, left for $b = 0.1$, right for $b = 0.3$).

where $\partial/\partial n_x$ is the directional derivative with respect to the outward normal direction at $\mathbf{x} \in \Gamma$. From the spirit of the MFS, the solution $u(\mathbf{x})$ is assumed to be [17–19]

$$u(\mathbf{x}) = \sum_{j=1}^{N} \alpha_j U_k(\mathbf{x}, \mathbf{s}_j) \tag{5}$$

where α_j is the intensity of *a priori* distributed source points at $\mathbf{s}_j$, and N is the number of source points. Then, we collocate Eq. (5) by satisfying the boundary condition in Eq. (1) at N boundary field points $\mathbf{x}_i$, it results in a

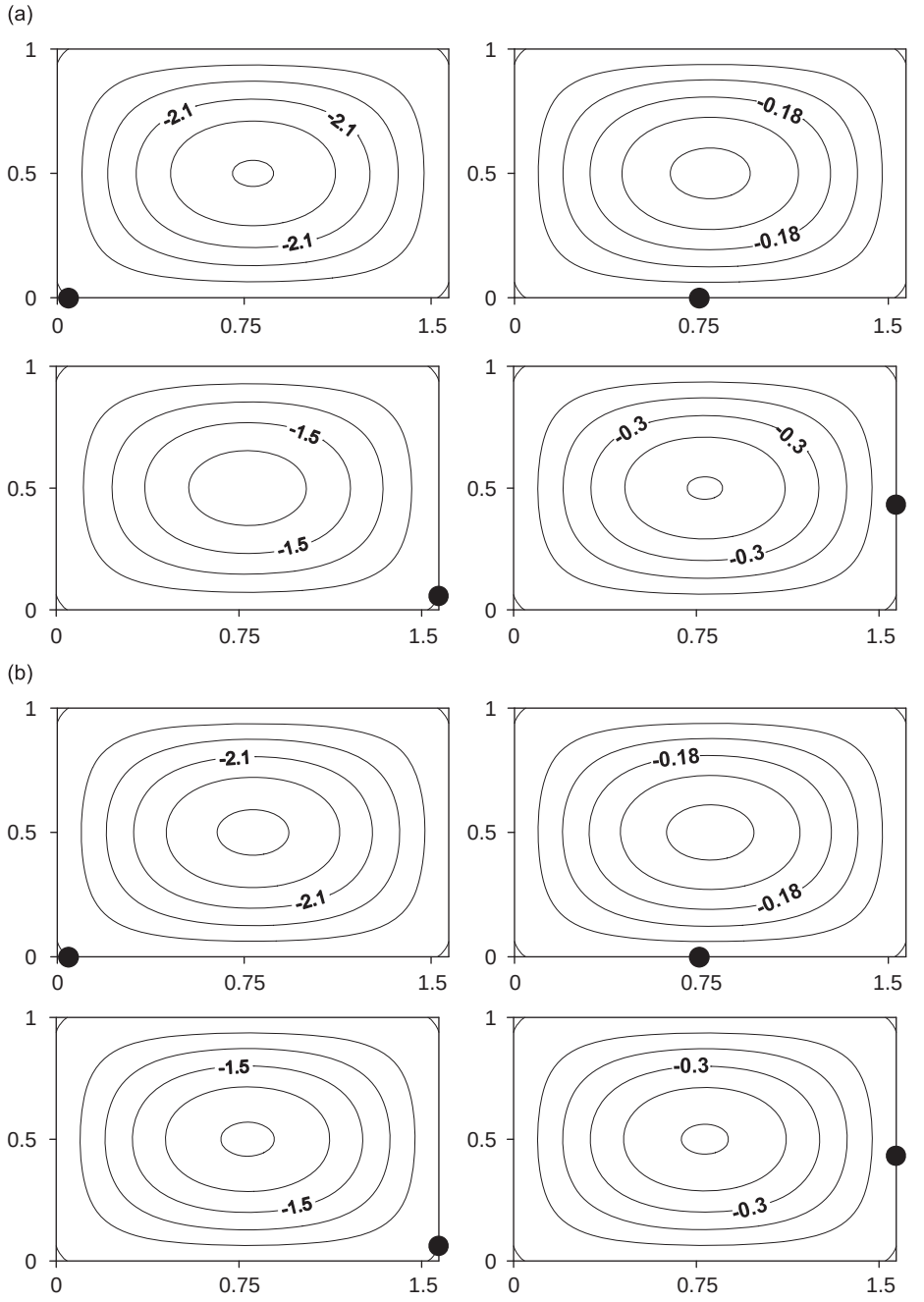

Fig. 4. Contours of the first eigenmode obtained by the linear LSMFS: (a) $b = 0.15$; (b) $b = 15$ (Example 1, $N = 52$).

$N \times N$ linear system with the same number of unknowns and equations:

$$\begin{bmatrix} A(k,\mathbf{x}_1,\mathbf{s}_1) & A(k,\mathbf{x}_1,\mathbf{s}_2) & \cdots & \cdots & A(k,\mathbf{x}_1,\mathbf{s}_N) \\ A(k,\mathbf{x}_2,\mathbf{s}_1) & A(k,\mathbf{x}_2,\mathbf{s}_2) & \cdots & \cdots & A(k,\mathbf{x}_2,\mathbf{s}_N) \\ \vdots & \vdots & \ddots & \ddots & \vdots \\ \vdots & \vdots & \ddots & \ddots & \vdots \\ A(k,\mathbf{x}_N,\mathbf{s}_1) & A(k,\mathbf{x}_N,\mathbf{s}_2) & \cdots & \cdots & A(k,\mathbf{x}_N,\mathbf{s}_N) \end{bmatrix} \begin{bmatrix} \alpha_1 \\ \alpha_2 \\ \vdots \\ \vdots \\ \alpha_N \end{bmatrix} = \begin{bmatrix} 0 \\ 0 \\ \vdots \\ \vdots \\ 0 \end{bmatrix} \tag{6}$$

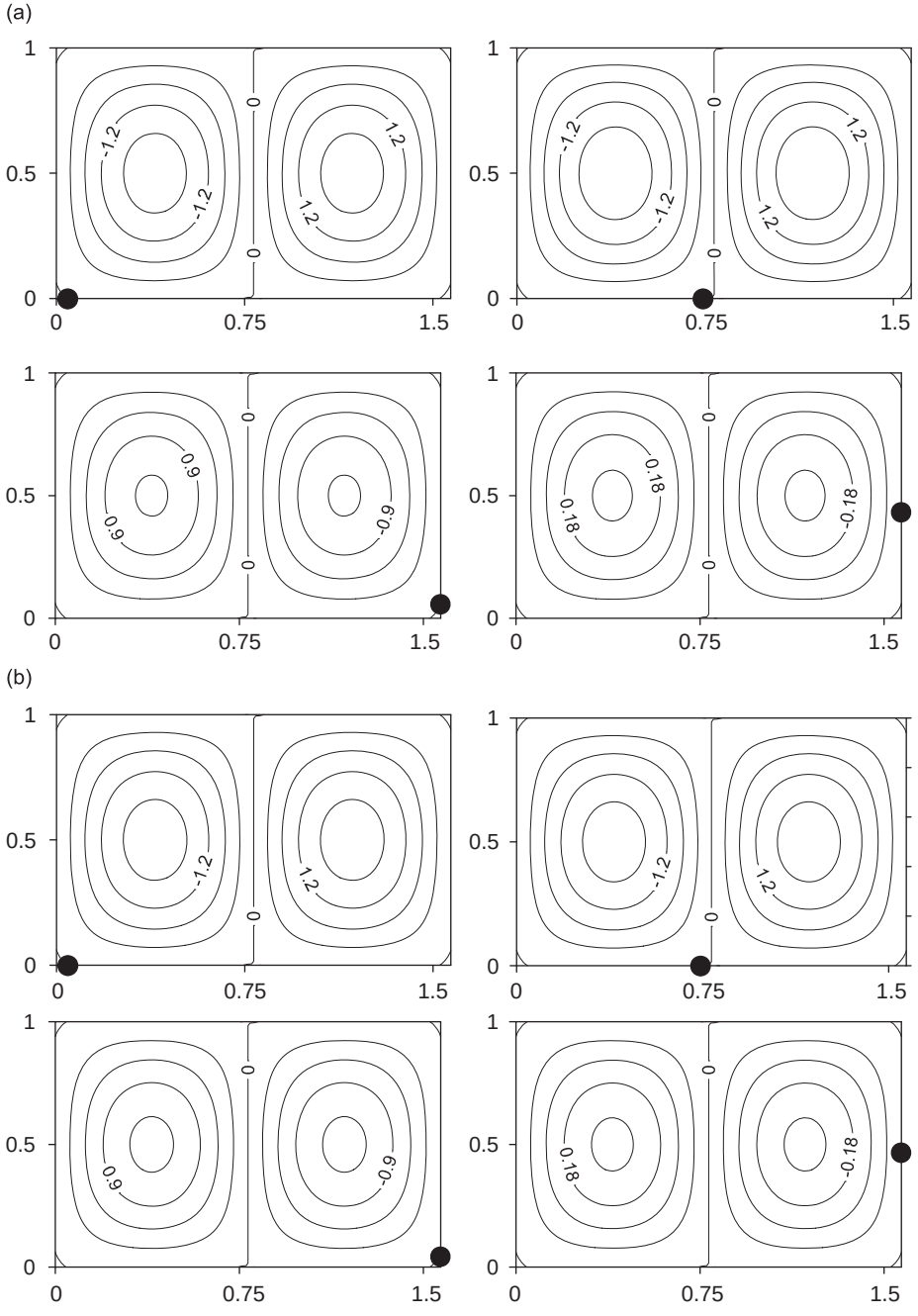

Fig. 5. Contours of the second eigenmode obtained by the linear LSMFS: (a) $b = 0.15$; (b) $b = 15$ (Example 1, $N = 52$).

where $A(k,\mathbf{x}_i,\mathbf{s}_j)=U_k(\mathbf{x}_i,\mathbf{s}_j)$ if $\mathbf{x}_i\in\Gamma^D$ and $A(k,\mathbf{x}_i,\mathbf{s}_j)=L_k(\mathbf{x}_i,\mathbf{s}_j)$ if $\mathbf{x}_i\in\Gamma^N$. In the present work, we uniformly distribute boundary field points and locate the source points by using the following formula [8,9,31]:

$$\mathbf{s}_i=\mathbf{x}_i+b\times(\mathbf{x}_i-\mathbf{x}_c) \tag{7}$$

where $\mathbf{x}_c$ are the spatial coordinates of the center of the computational domain and b is a spatial parameter as depicted in Fig. 1(b). Once the parameter b is chosen, the distributions of the source points can be obtained from the above equation. Eq. (6) is a nonlinear eigenproblem for k that we are searching for eigenvalues $k_1<k_2<k_3<\cdots$ such that Eq. (6) has nontrivial solutions. In the present work, we adopted the direct

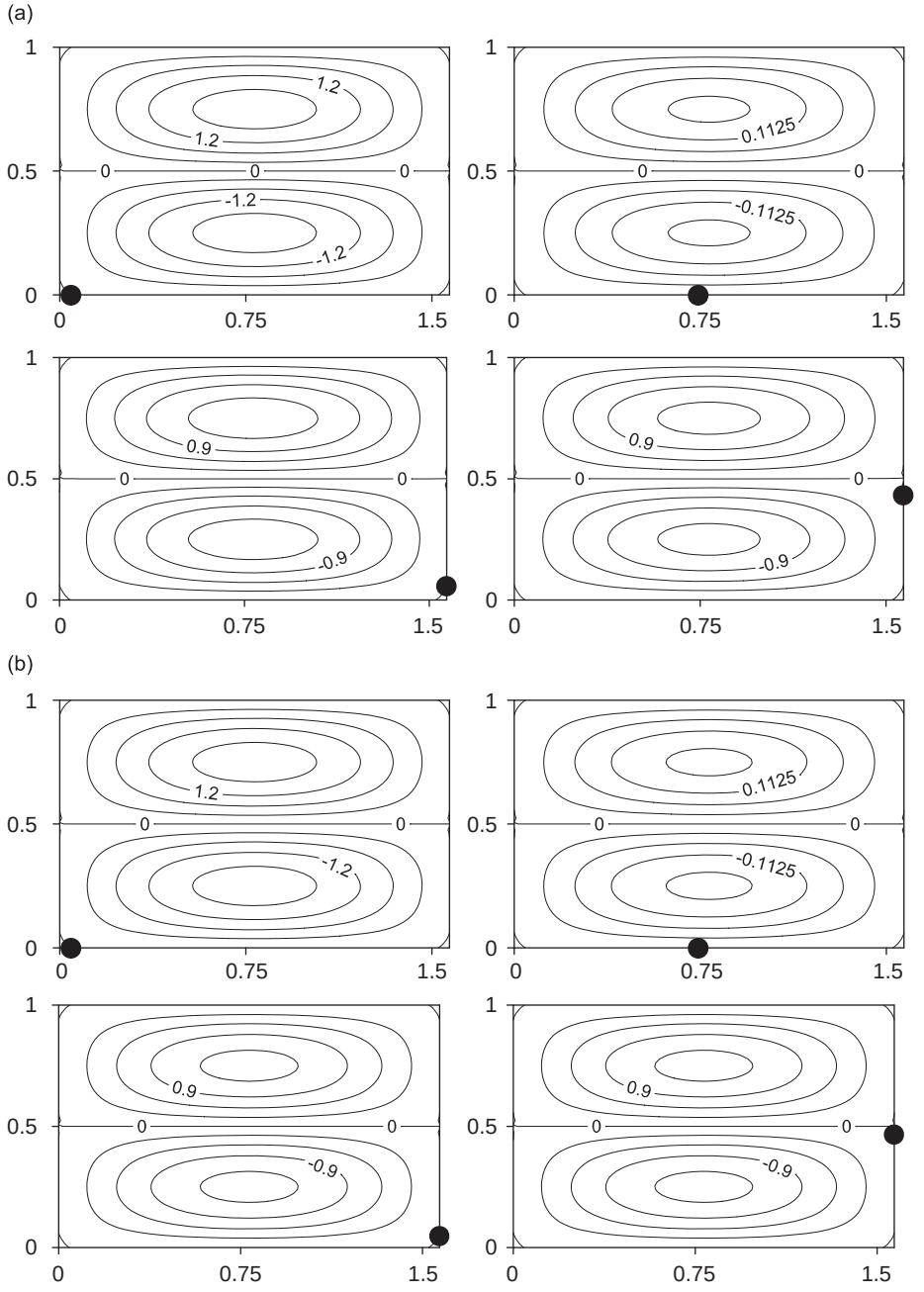

Fig. 6. Contours of the third eigenmode obtained by the linear LSMFS: (a) $b=0.15$; (b) $b=15$ (Example 1, $N=52$).

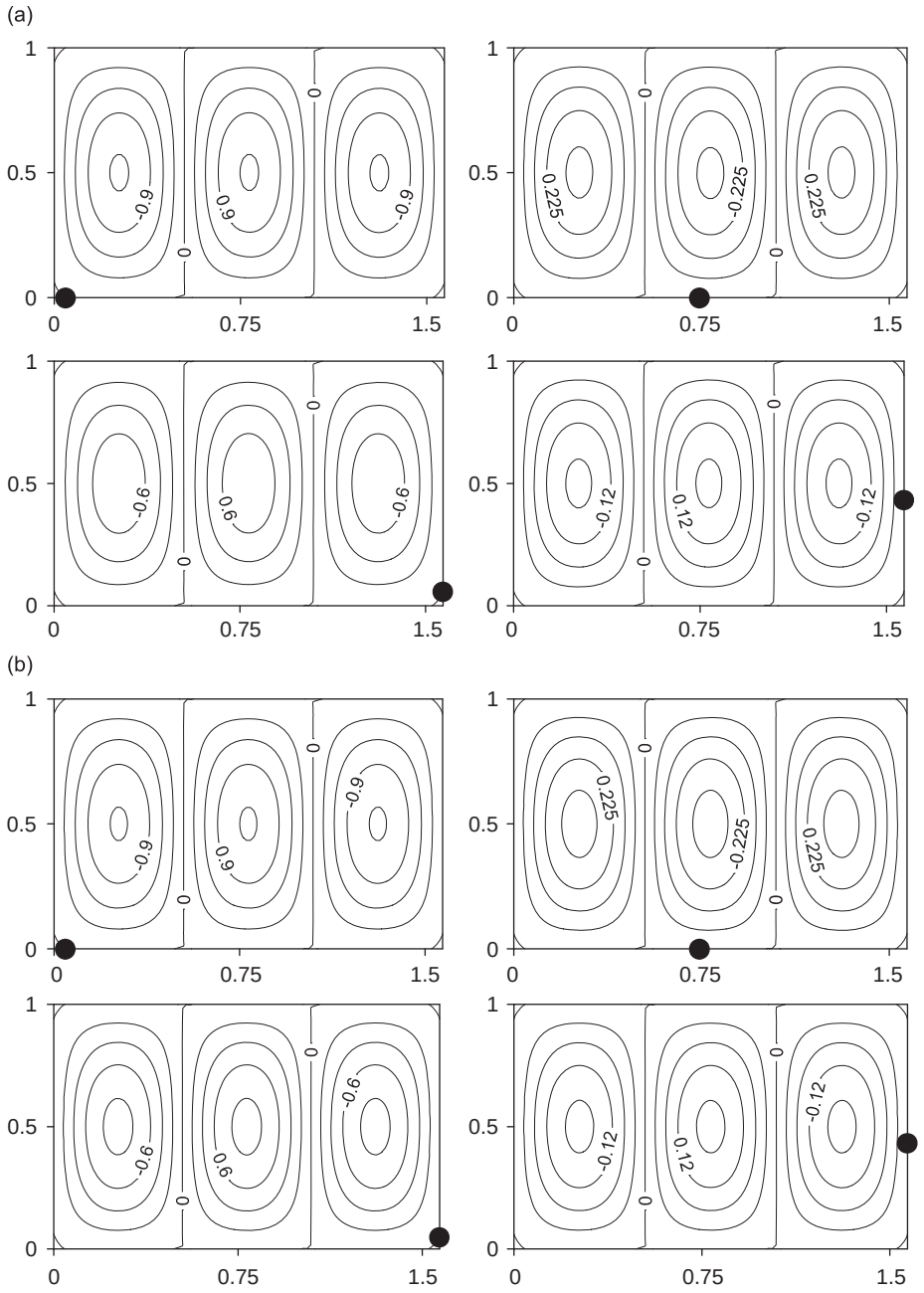

Fig. 7. Contours of the fourth eigenmode obtained by the linear LSMFS: (a) $b = 0.15$; (b) $b = 15$ (Example 1, $N = 52$).

Table 4
The four lowest eigenvalues for different nodes (Example 2, $b = 0.8$).

	Analytic solution	$N = 28$	$N = 36$	$N = 44$	$N = 52$	$N = 60$
Mode 1	3.1415927	3.141647	3.141586	3.141594	3.141593	3.141593
Mode 2	4.4428829	4.442951	4.442881	4.442881	4.442883	4.442883
Mode 3	6.2831853	6.283186	6.283185	6.283185	6.283185	6.283185
Mode 4	7.0248147	7.024558	7.024865	7.024810	7.024816	7.024815

Table 5
The four lowest eigenvalues for different locations of source points (Example 2, $N = 52$).

	Analytic solution	$b = 0.15$	$b = 0.2$	$b = 0.5$	$b = 0.8$	$b = 2.0$
Mode 1	3.1415927	3.140530	3.141664	3.141590	3.141593	3.141592
Mode 2	4.4428829	4.442166	4.442893	4.442892	4.442883	4.442883
Mode 3	6.2831853	6.283504	6.283296	6.283185	6.283185	6.283185
Mode 4	7.0248147	7.025631	7.024734	7.024830	7.024816	7.024815

Table 6
The four lowest eigenvalues for different nodes (Example 2, by FEM).

	Analytic solution	$N = 400$	$N = 900$	$N = 1600$	$N = 2500$	$N = 3600$
Mode 1	3.141593	3.14481	3.14303	3.14240	3.14211	3.14195
Mode 2	4.442883	4.45651	4.44896	4.44630	4.44507	4.44440
Mode 3	6.283185	6.30898	6.29466	6.28964	6.28732	6.28605
Mode 4	7.024815	7.06166	7.04128	7.03410	7.03075	7.02895

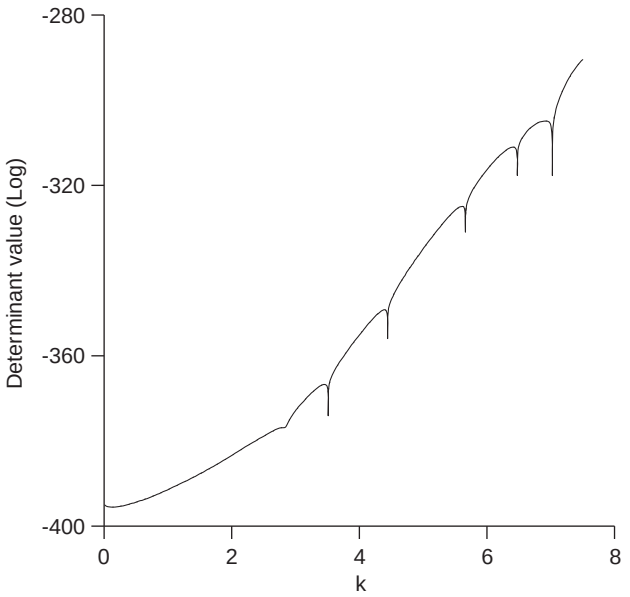

Fig. 8. The result of the direct determinant search method (Example 2).

determinant search method to find the associated eigenvalues [17–19]. After eigenvalues are obtained, we can solve the corresponding eigenvectors $\{\alpha_j\}(k_1), \{\alpha_j\}(k_2), \{\alpha_j\}(k_3), \ldots$ by utilizing the SVD [26,27]. Intuitively, we are able to find the numerical eigenfunctions, $u(\mathbf{x})(k_1), u(\mathbf{x})(k_2), u(\mathbf{x})(k_3), \ldots$of the original Helmholtz equation, Eq. (1), by applying Eq. (5). However, it is found that the mode shapes are sensitive with respect to the locations of sources.

To circumvent this difficulty, an alternative method is thus developed. Assume $k = k'$ is an eigenvalue of Eq. (1) and $\mathbf{x}^D \in \Gamma$ is a specific boundary point. We seek for α_j that minimizes the following functional [30]:

$$S(\alpha_j) = \sum_{i=1}^{N} \left| \begin{cases} \sum_{j=1}^{N} \alpha_j U_{k'}(\mathbf{x}_i, \mathbf{s}_j) & \text{if } \mathbf{x}_i \in \Gamma^D \\ \sum_{j=1}^{N} \alpha_j L_{k'}(\mathbf{x}_i, \mathbf{s}_j) & \text{if } \mathbf{x}_i \in \Gamma^N \end{cases} \right|^2 + \left| 1 - \begin{cases} \sum_{j=1}^{N} \alpha_j L_{k'}(\mathbf{x}_i, \mathbf{s}_j) & \text{if } \mathbf{x}^D \in \Gamma^D \\ \sum_{j=1}^{N} \alpha_j U_{k'}(\mathbf{x}_i, \mathbf{s}_j) & \text{if } \mathbf{x}^D \in \Gamma^N \end{cases} \right|^2 \tag{8}$$

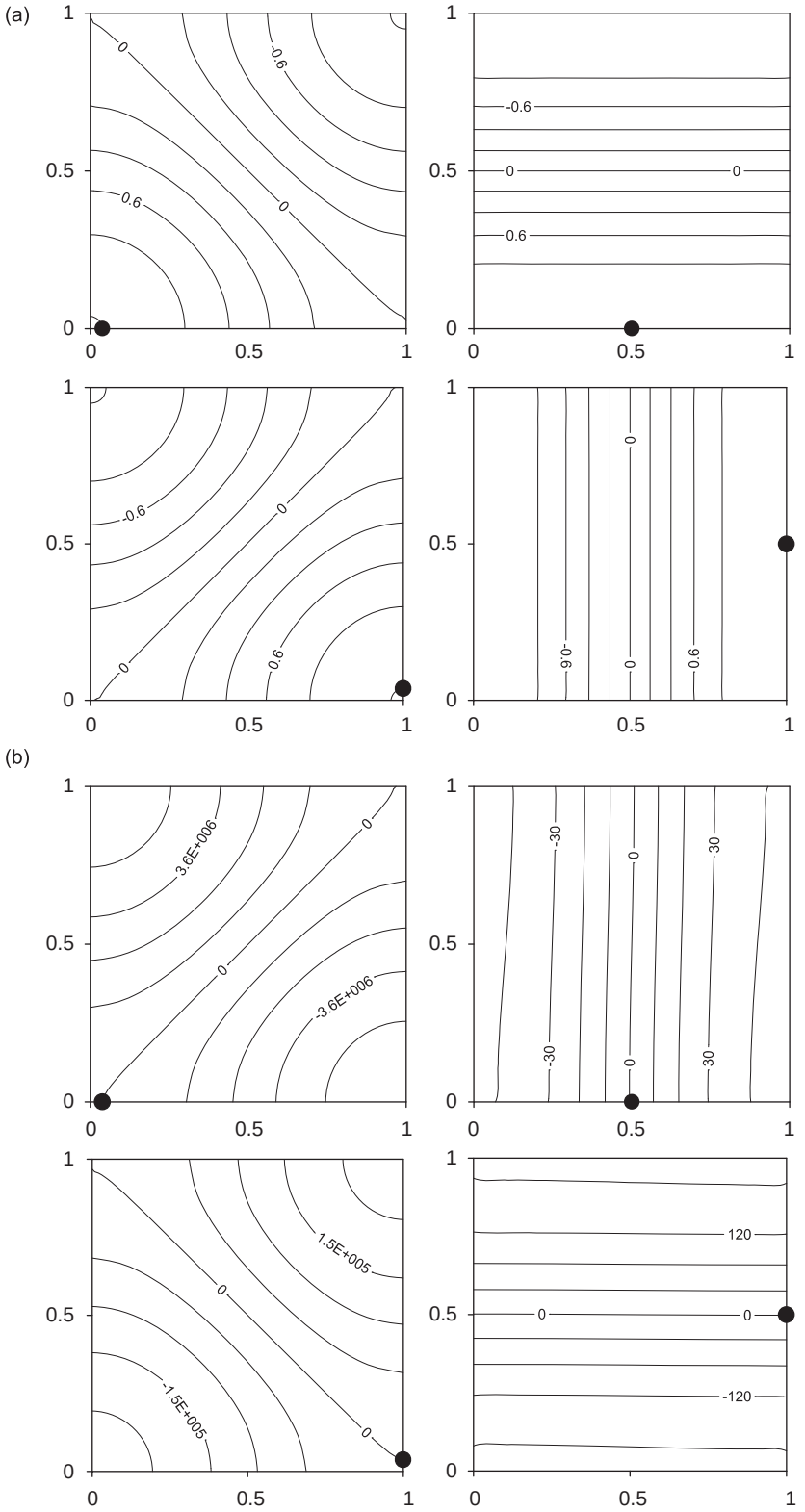

Fig. 9. Contours of the first eigenmode obtained by the linear LSMFS: (a) $b = 0.15$; (b) $b = 15$ (Example 2, $N = 52$).

The minimization of the functional in Eq. (8) is equivalent to the least squares solution of the following system of linear equations:

$$\begin{bmatrix} A(k',\mathbf{x}_1,\mathbf{s}_1) & A(k',\mathbf{x}_1,\mathbf{s}_2) & \cdots & \cdots & A(k',\mathbf{x}_1,\mathbf{s}_N) \\ A(k',\mathbf{x}_2,\mathbf{s}_1) & A(k',\mathbf{x}_2,\mathbf{s}_2) & \cdots & \cdots & A(k',\mathbf{x}_2,\mathbf{s}_N) \\ \vdots & \vdots & \ddots & \ddots & \vdots \\ \vdots & \vdots & \ddots & \ddots & \vdots \\ A(k',\mathbf{x}_N,\mathbf{s}_1) & A(k',\mathbf{x}_N,\mathbf{s}_2) & \cdots & \cdots & A(k',\mathbf{x}_N,\mathbf{s}_N) \\ B(k',\mathbf{x}^D,\mathbf{s}_1) & B(k',\mathbf{x}^D,\mathbf{s}_2) & \cdots & \cdots & B(k',\mathbf{x}^D,\mathbf{s}_N) \end{bmatrix} \begin{bmatrix} \alpha_1 \\ \alpha_2 \\ \vdots \\ \vdots \\ \alpha_N \end{bmatrix} = \begin{bmatrix} 0 \\ 0 \\ \vdots \\ \vdots \\ 0 \\ b_1 \end{bmatrix} \tag{9}$$

where $A(k',\mathbf{x}_i,\mathbf{s}_j) = U_{k'}(\mathbf{x}_i,\mathbf{s}_j)$ if $\mathbf{x}_i \in \Gamma^D$ and $A(k',\mathbf{x}_i,\mathbf{s}_j) = L_{k'}(\mathbf{x}_i,\mathbf{s}_j)$ if $\mathbf{x}_i \in \Gamma^N$ as well as $B(k',\mathbf{x}^D,\mathbf{s}_j) = L_{k'}(\mathbf{x}^D,\mathbf{s}_j)$ if $\mathbf{x}^D \in \Gamma^D$ and $B(k',\mathbf{x}^D,\mathbf{s}_j) = U_{k'}(\mathbf{x}^D,\mathbf{s}_j)$ if $\mathbf{x}^D \in \Gamma^N$. b_1 is an arbitrary constant other than zero. In this paper, $b_1 = 1$ is typically selected. Therefore, the mode shape corresponding to $k = k'$ by specifying a normalized dual boundary condition at $\mathbf{x}^D$ can thus be obtained by utilizing Eq. (5) after α_j are obtained by using Eq. (9).

Furthermore, in order to normalize the modal contours for eigenmodes with degeneracy of multiplicity 2, two dual boundary conditions at $\mathbf{x}_1^D$ and $\mathbf{x}_2^D$ are thus imposed. Therefore, the linear LSMFS can be presented

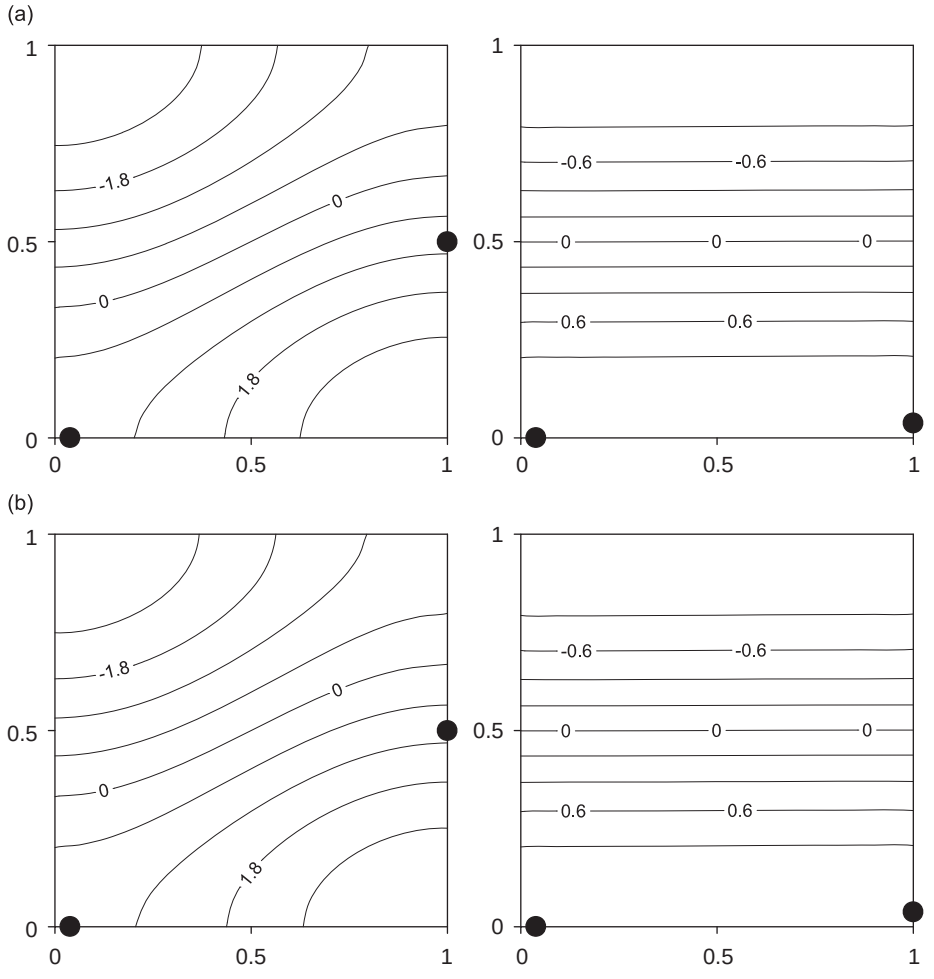

Fig. 10. Contours of the degenerate eigenmode after normalization: (a) $b = 0.15$; (b) $b = 15$ (Example 2, modes 1, $N = 52$).

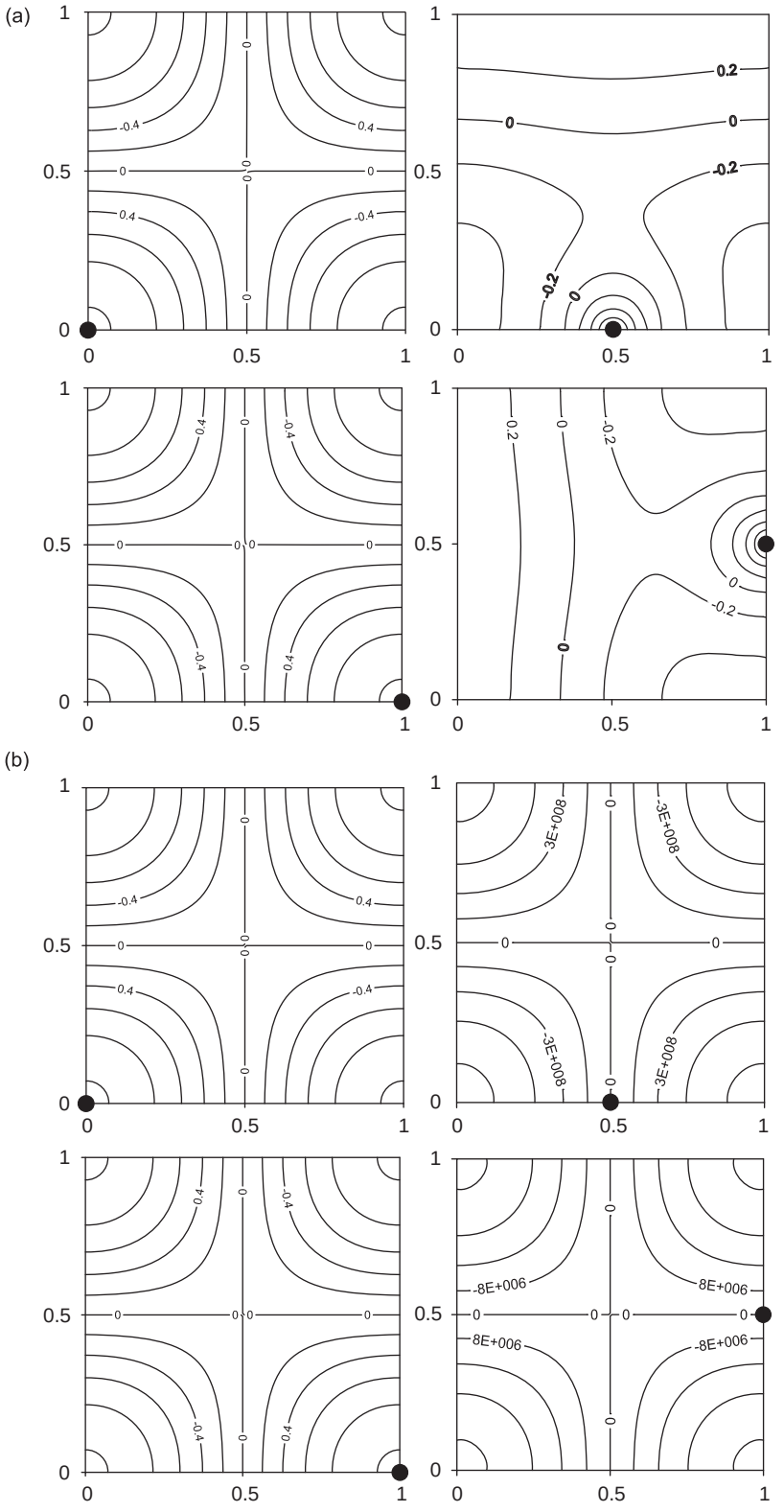

Fig. 11. Contours of the second eigenmode obtained by the linear LSMFS: (a) $b = 0.15$; (b) $b = 15$ (Example 2, $N = 52$).

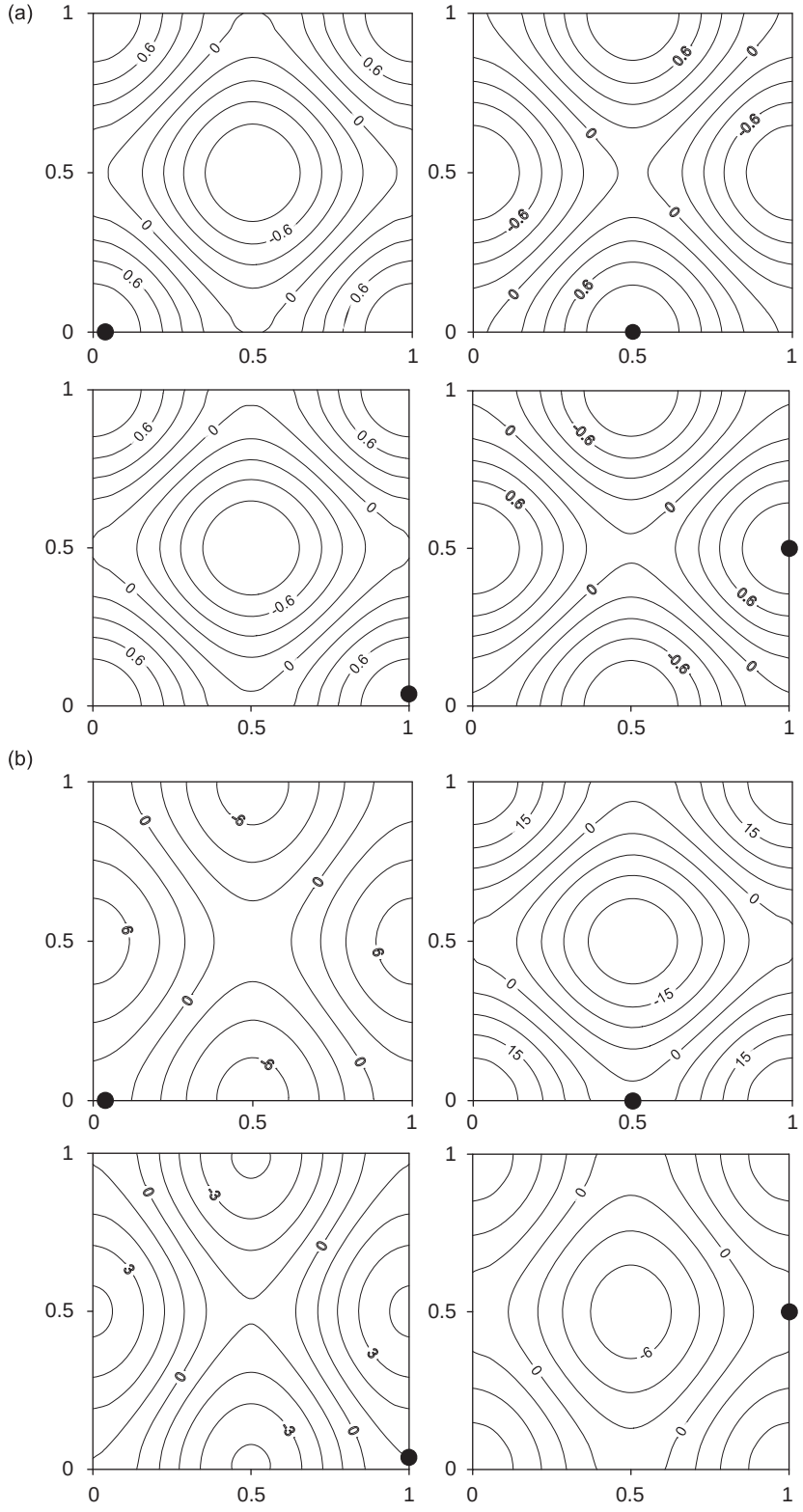

Fig. 12. Contours of the third eigenmode obtained by the linear LSMFS: (a) $b = 0.15$; (b) $b = 15$ (Example 2, $N = 52$).

by the following matrix form with similar notations:

$$\begin{bmatrix} A(k',\mathbf{x}_1,\mathbf{s}_1) & A(k',\mathbf{x}_1,\mathbf{s}_2) & \cdots & \cdots & A(k',\mathbf{x}_1,\mathbf{s}_N) \\ A(k',\mathbf{x}_2,\mathbf{s}_1) & A(k',\mathbf{x}_2,\mathbf{s}_2) & \cdots & \cdots & A(k',\mathbf{x}_2,\mathbf{s}_N) \\ \vdots & \vdots & \ddots & \ddots & \vdots \\ \vdots & \vdots & \ddots & \ddots & \vdots \\ A(k',\mathbf{x}_N,\mathbf{s}_1) & A(k',\mathbf{x}_N,\mathbf{s}_2) & \cdots & \cdots & A(k',\mathbf{x}_N,\mathbf{s}_N) \\ B(k',\mathbf{x}_1^D,\mathbf{s}_1) & B(k',\mathbf{x}_1^D,\mathbf{s}_2) & \cdots & \cdots & B(k',\mathbf{x}_1^D,\mathbf{s}_N) \\ B(k',\mathbf{x}_2^D,\mathbf{s}_1) & B(k',\mathbf{x}_2^D,\mathbf{s}_2) & \cdots & \cdots & B(k',\mathbf{x}_2^D,\mathbf{s}_N) \end{bmatrix} \begin{bmatrix} \alpha_1 \\ \alpha_2 \\ \vdots \\ \vdots \\ \alpha_N \end{bmatrix} = \begin{bmatrix} 0 \\ 0 \\ \vdots \\ \vdots \\ 0 \\ c_1 \\ c_2 \end{bmatrix} \tag{10}$$

where c_1 and c_2 are two arbitrary constants whose selections will be described in the next section.

3. Numerical results

In order to validate the proposed numerical method, two numerical experiments of Dirichlet problem without degeneracy and Neumann problems with degenerate modes are first considered. Then the method is

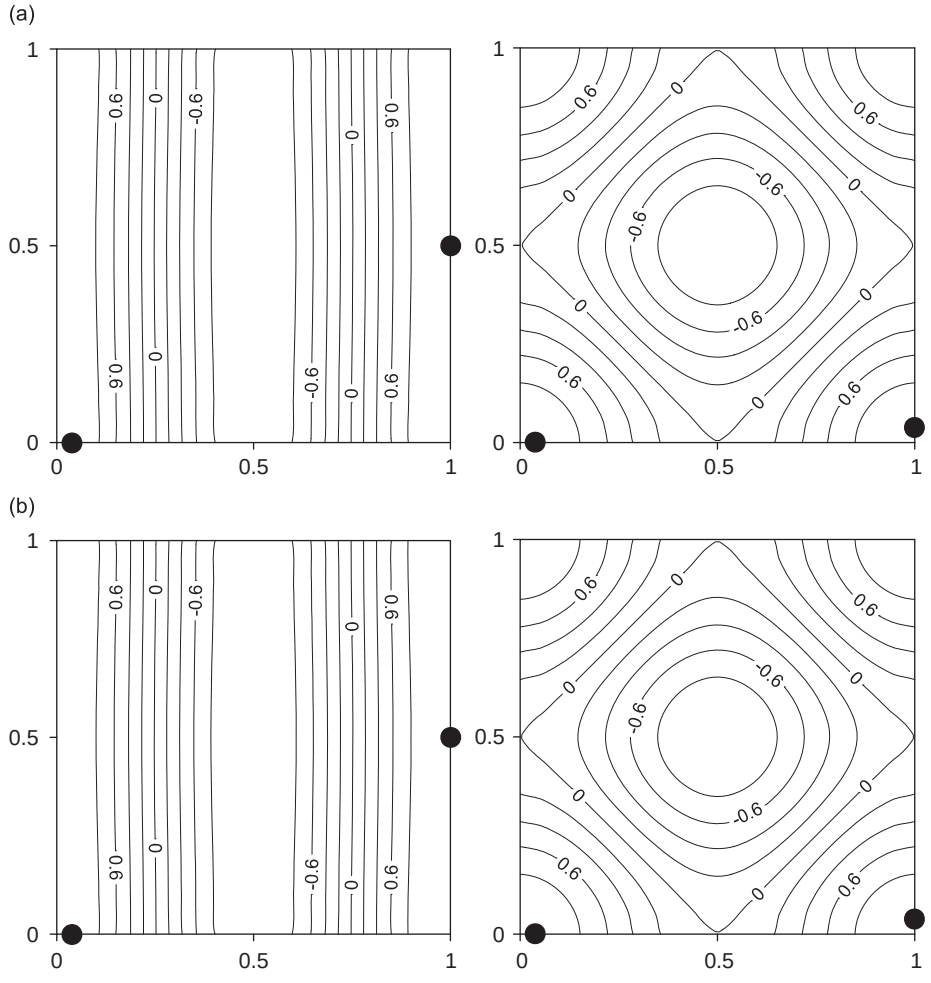

Fig. 13. Contours of the degenerate eigenmode after normalization: (a) $b = 0.15$; (b) $b = 15$ (Example 2, modes 3, $N = 52$).

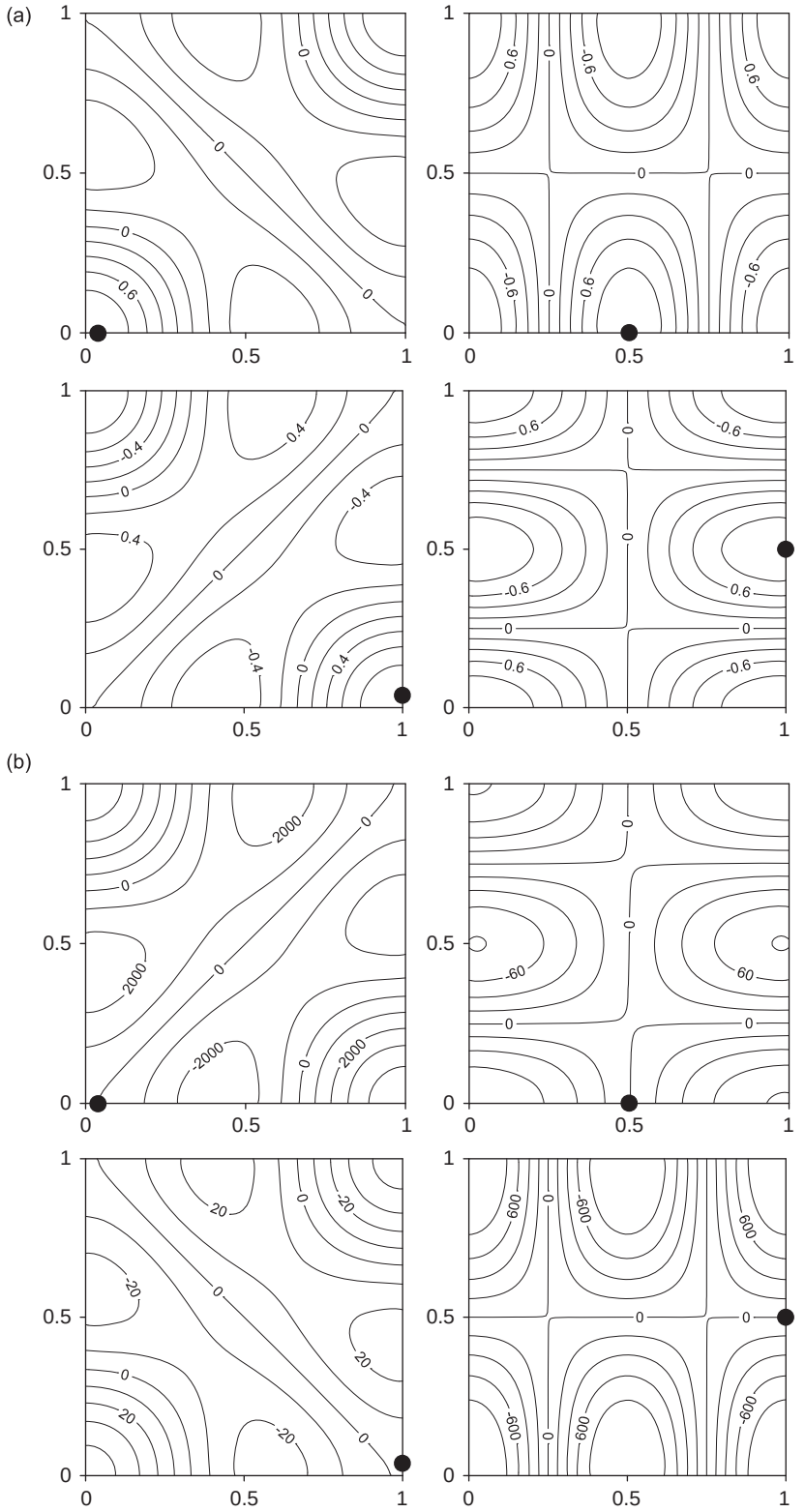

Fig. 14. Contours of the fourth eigenmode obtained by the linear LSMFS: (a) $b = 0.15$; (b) $b = 15$ (Example 2, $N = 52$).

applied to solve a practical problem in complex domain without exact solution. The high accuracy of the eigenvalues obtained by the linear LSMFS are demonstrated and compared with those obtained by the FEM. Furthermore, we will show the robustness of obtaining mode shapes by utilizing the linear LSMFS. The failure in determining the mode shapes by specifying a normalized data at the point near or on the nodes are examined, and it is found that the degenerate eigenmodes can be distinguished by specifying the boundary data at different boundary points. The normalized contours of degenerate eigenmodes, obtained by specifying two dual boundary data, are also sketched for different locations of source points.

3.1. Example 1: Dirichlet problem without degeneracy

In the first example, we consider the following acoustical problem with Dirichlet boundary condition:

$$\begin{cases} (\nabla^2 + k^2)u(\mathbf{x}) = 0, & \mathbf{x} \in \left\{(x,y)\middle|0 \leqslant x \leqslant \frac{\pi}{2} \cap 0 \leqslant y \leqslant 1\right\} \\ u(\mathbf{x}) = 0, & \mathbf{x} \in \left\{(x,y)\middle|\left(x = 0, \frac{\pi}{2} \cap 0 \leqslant y \leqslant 1\right) \cup \left(y = 0, 1 \cap 0 \leqslant x \leqslant \frac{\pi}{2}\right)\right\} \end{cases} \tag{11}$$

The four lowest eigenvalues obtained by the direct determinant search method applying to the matrix in Eq. (6) are given in Tables 1 and 2, respectively, for different nodes (N) by fixed locations of source points (b)

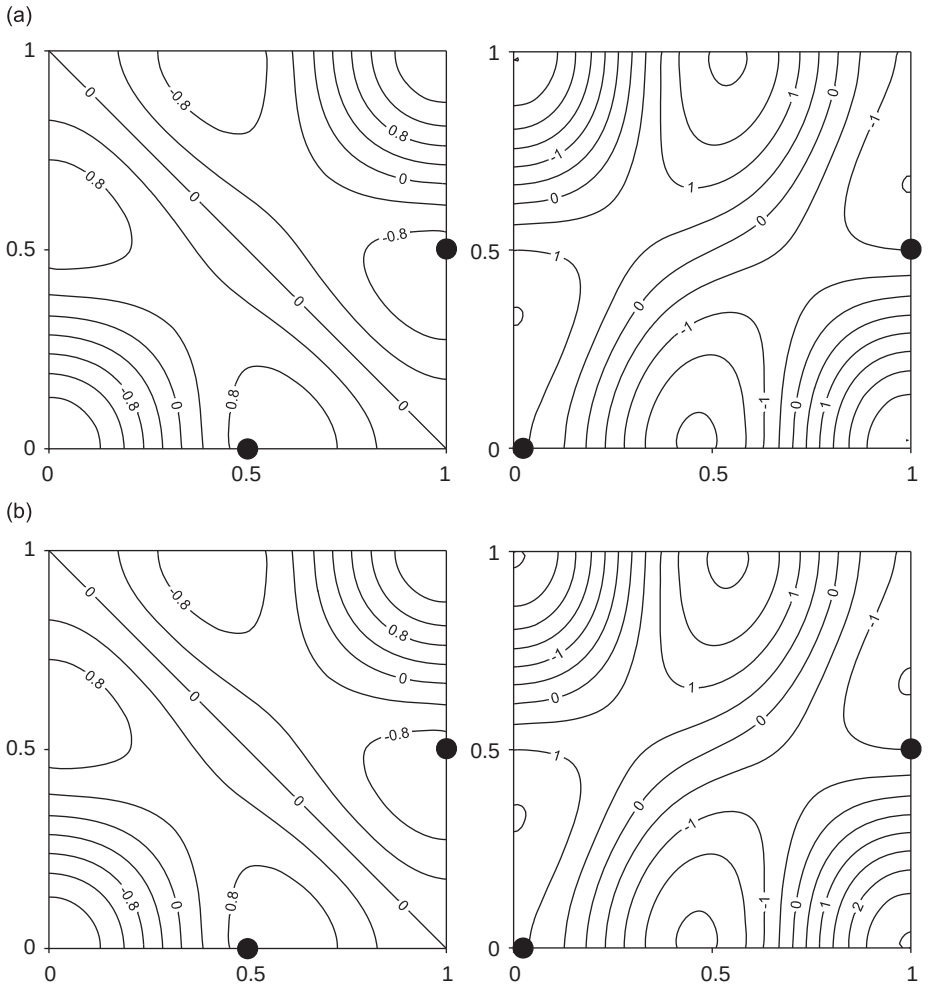

Fig. 15. Contours of the degenerate eigenmode after normalization: (a) $b = 0.15$; (b) $b = 15$ (Example 2, modes 4, $N = 52$).

and different locations of source points by fixed nodes. From Tables 1 and 2, we can observe rapid convergent behaviors of eigenvalues as b and N become larger. The numerical eigenvalues are generally accurate up to 10^{-5} compared with the exact solutions. Table 1 reveals that the larger number of nodes gives the better accuracy. Also, it is observed that the eigenvalues are not sensitive to the locations of source points, even as b is close to zero, $b = 0.0001$. These results are much better than those obtained by the FEM as reported in Table 3, in which a large number of nodes are required to obtain the same order of accurate eigenvalues. Fig. 2 depicts an example plot of the direct determinant search method. It is thus convinced that the MFS in conjunction with the direct determinant search method is capable to obtain eigenvalues robustly and accurately as stated in the literature [17–19].

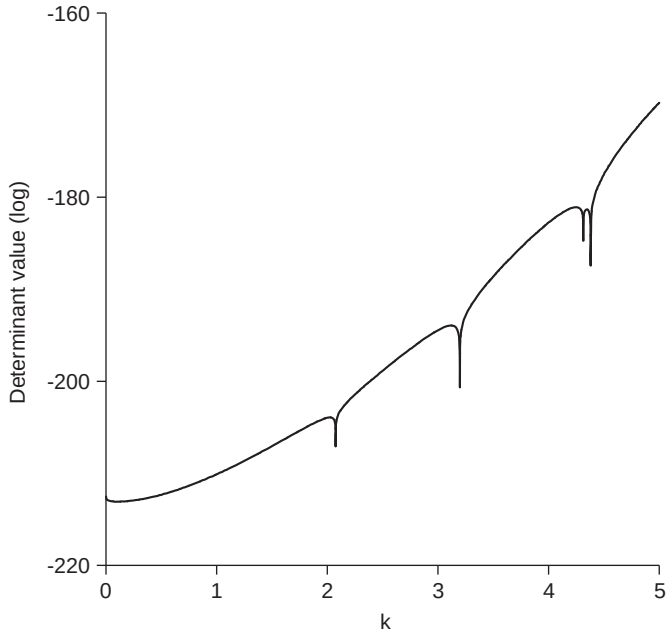

Fig. 16. The result of the direct determinant search method (Example 3).

Table 7
The four lowest eigenvalues for different nodes (Example 3, $b = 0.8$).

	$N = 24$	$N = 36$	$N = 48$	$N = 60$	$N = 72$
Mode 1	2.07550	2.07539	2.07539	2.07539	2.07539
Mode 2	3.19844	3.19862	3.19864	3.19864	3.19864
Mode 3	4.31387	4.31420	4.31424	4.31424	4.31424
Mode 4	4.38148	4.38134	4.38138	4.38138	4.38138

Table 8
The four lowest eigenvalues for different locations of source points (Example 3, $N = 60$).

	$b = 0.01$	$B = 0.1$	$b = 0.2$	$b = 0.5$	$b = 0.8$	$b = 2.0$
Mode 1	2.04257	2.07549	2.07539	2.07539	2.07539	2.07539
Mode 2	3.14671	3.19888	3.19864	3.19864	3.19864	3.19864
Mode 3	4.24455	4.31460	4.31424	4.31424	4.31424	4.31421
Mode 4	4.31221	4.38161	4.38138	4.38138	4.38138	4.38138

The numerical results also explain why solving mode shapes is the subject of research focused in this study. Fig. 3 indicates the mode shapes obtained for different locations of source points by applying the SVD to the matrix in Eq. (6). The SVD can provide the reasonable mode shapes, when the value of b is taken as 0.1. It is known that farther sources will give better accuracy but worse conditioning in the application of MFS [3,4,28]. As a result, the ill-conditioning makes the SVD scheme fail to determine the eigenmodes when b is increased to 0.3.

On the other hand, by specifying a normalized dual boundary data at the different boundary locations, the mode shapes of acoustical modes obtained by the linear LSMFS (Eq. (9)) for different locations of source

Table 9
The four lowest eigenvalues for different nodes (Example 3, by FEM).

	$N = 2000$	$N = 3000$	$N = 4000$	$N = 5000$	$N = 10000$
Mode 1	2.07630	2.07604	2.07586	2.07578	2.07558
Mode 2	3.20188	3.20091	3.20028	3.20001	3.19931
Mode 3	4.32214	4.31975	4.31827	4.31759	4.31586
Mode 4	4.38978	4.38697	4.38548	4.38473	4.38304

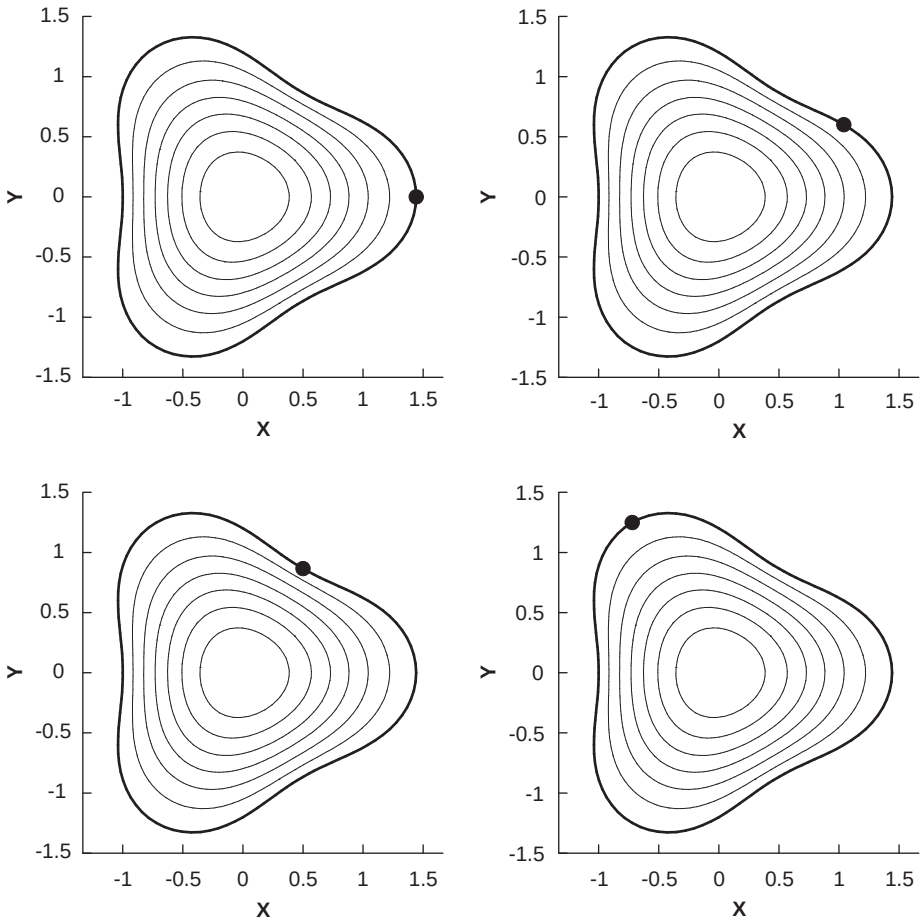

Fig. 17. Contours of the first eigenmode obtained by the linear LSMFS (Example 3, $b = 0.8$ and $N = 60$).

points are depicted in Figs. 4–7, where the dark circle "●" denotes the specified position of the normalized boundary data. In these figures, the acoustical modes are almost the same in shape since all eigenmodes are not degenerate. Unlike the mode shapes are sensitive to the locations of source points by utilizing the SVD, the proposed method is really robust with respect to the spatial parameter b. Based on these numerical results, it is convinced that the linear LSMFS is capable of determining the mode shapes of acoustical eigenmodes.

3.2. Example 2: Neumann problem with degeneracy

To demonstrate the capability of the present method for degenerate modes, we next consider the square cavity with the Neumann boundary condition:

$$\begin{cases} (\nabla^2 + k^2)u(\mathbf{x}) = 0, & \mathbf{x} \in \{(x,y)|0 \leqslant x \leqslant 1 \cap 0 \leqslant y \leqslant 1\} \\ \dfrac{\partial u(\mathbf{x})}{\partial n} = 0, & \mathbf{x} \in \{(x,y)|(x=0,1 \cap 0 \leqslant y \leqslant 1) \cup (y=0,1 \cap 0 \leqslant x \leqslant 1)\} \end{cases} \tag{12}$$

Similarly, the four lowest eigenvalues obtained by the direct determinant search method are stated in Tables 4 and 5 for different nodes (N) and locations of source points (b), respectively. Rapid convergent behaviors of eigenvalues can also be observed as b and N become larger. In addition, these results are much more accurate than those obtained by the FEM as exhibited in Table 6, where a lot of nodes are required to obtain accurate eigenvalues. Similarly, an example plot of the direct determinant search method is depicted in Fig. 8. In these

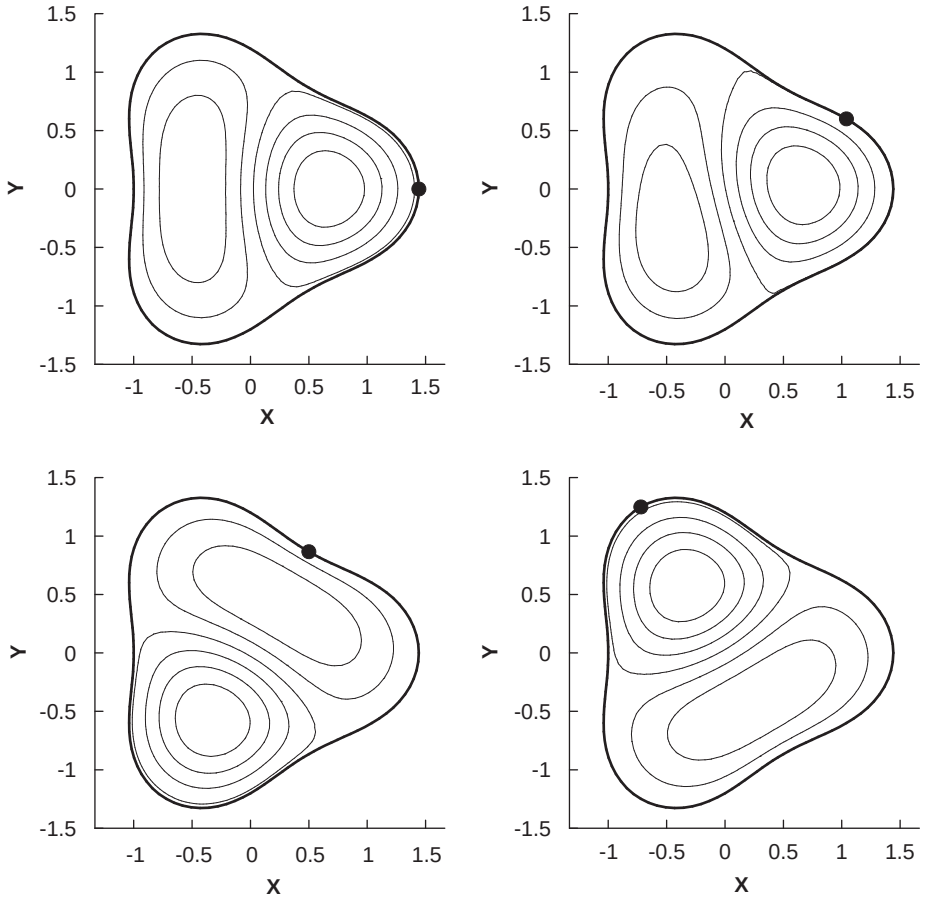

Fig. 18. Contours of the second eigenmode obtained by the linear LSMFS (Example 3, $b = 0.8$ and $N = 60$).

numerical experiments, it is noticed that accurate eigenvalues are obtained only for $b \geqslant 0.15$ since the singularities are stronger for Neumann problems. Overall, it is also convinced that accurate eigenfrequencies can be obtained robustly by using the linear LSMFS.

Furthermore, the mode shapes of acoustical eigenmodes solved by the linear LSMFS (Eq. (9)) for different locations of source points are depicted in Figs. 9–15. For the case of nondegenerate modes (Fig. 11), the mode shapes are almost the same in shape except the specified normalized data at the boundary locations near or on the nodes ($u = 0$). For the larger value of b ($b = 15$), these failures disappear. The contours have extremely large values since farther sources will give higher accuracy, thus small numerical differences can be distinguished. On the other hand, for the cases of degenerate modes (Figs. 9, 12 and 14), the mode shapes vary with respect to the positions of the specified normalized boundary data. Furthermore, the normalized contours obtained by specifying two dual boundary data (Eq. (10)) are also demonstrated in Figs. 10, 13 and 15, which also show the insensitivity on the locations of source points. The constants (c_1, c_2) in Eq. (10) are assumed to be units in Figs. 10 and 13. In order to demonstrate the influence of these constants, the results for $c_1 = 1$ and $c_2 = 2$ are depicted in Fig. 15. Thus, it is convinced that the linear LSMFS is able to obtain mode shapes for degenerate eigenmodes robustly.

3.3. Example 3: Dirichlet problem in a complex domain

Finally, we consider a more practical problem with Dirichlet boundary condition in the domain defined by

$$\rho = (\cos 3\theta + \sqrt{4 - \sin^2 3\theta})^{1/3}, \quad 0 \leqslant \theta \leqslant 2\pi \tag{13}$$

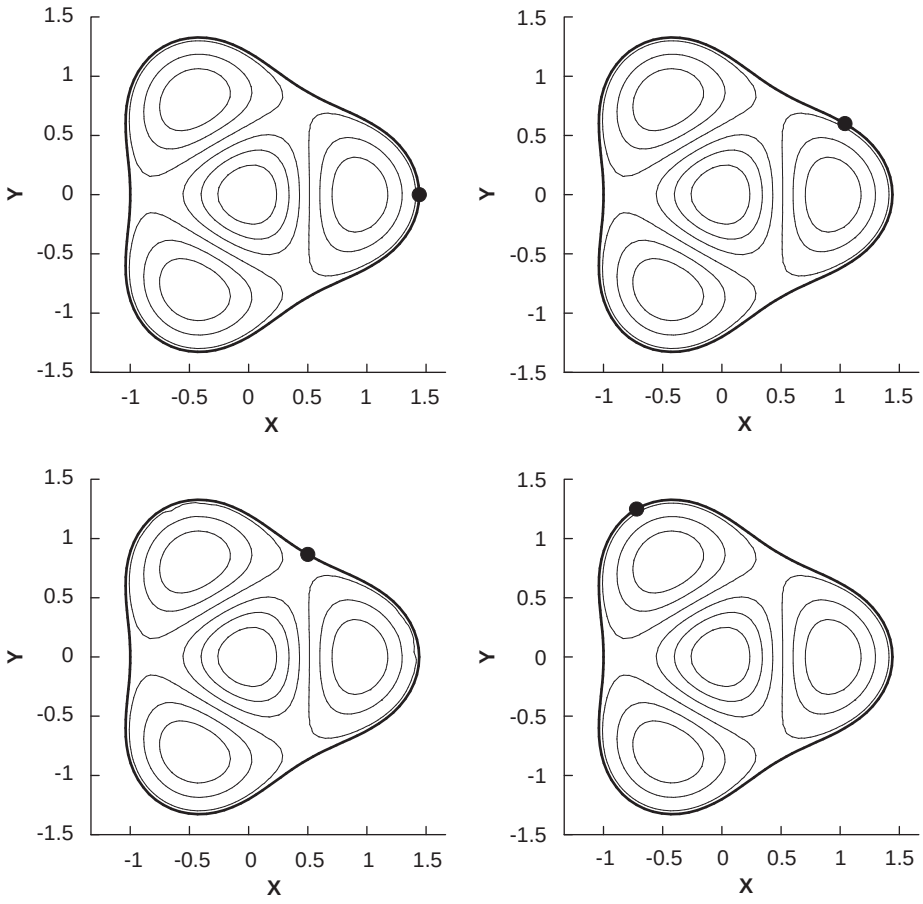

Fig. 19. Contours of the third eigenmode obtained by the linear LSMFS (Example 3, $b = 0.8$ and $N = 60$).

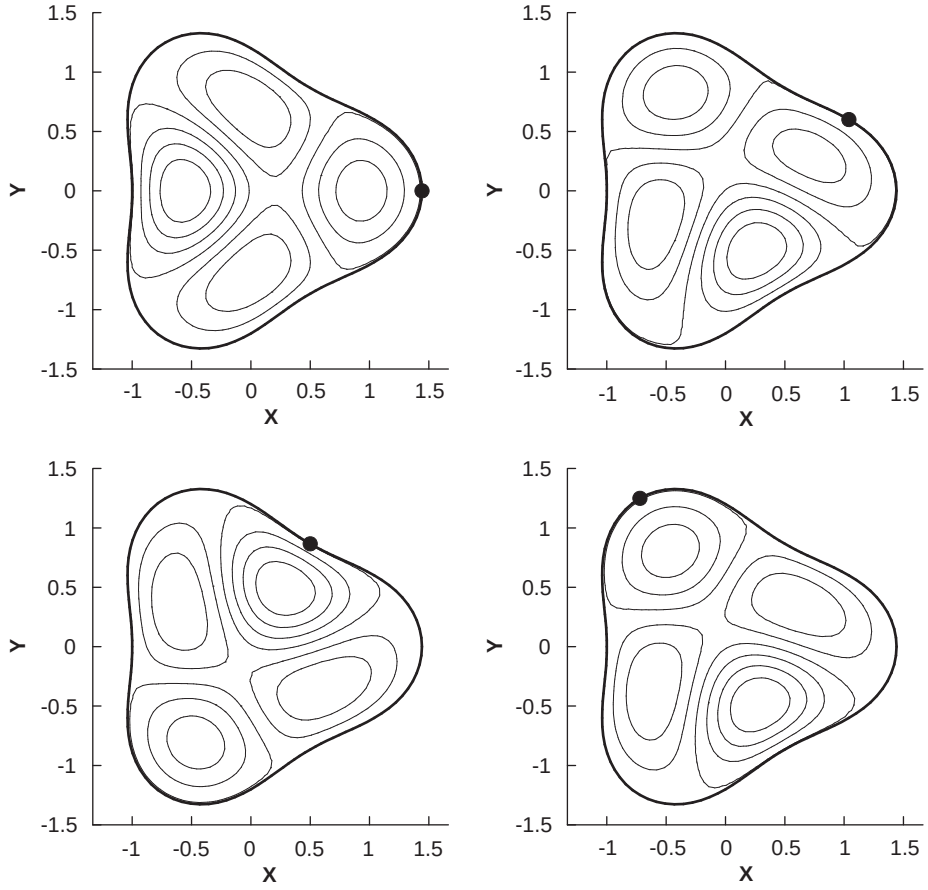

Fig. 20. Contours of the fourth eigenmode obtained by the linear LSMFS (Example 3, $b = 0.8$ and $N = 60$).

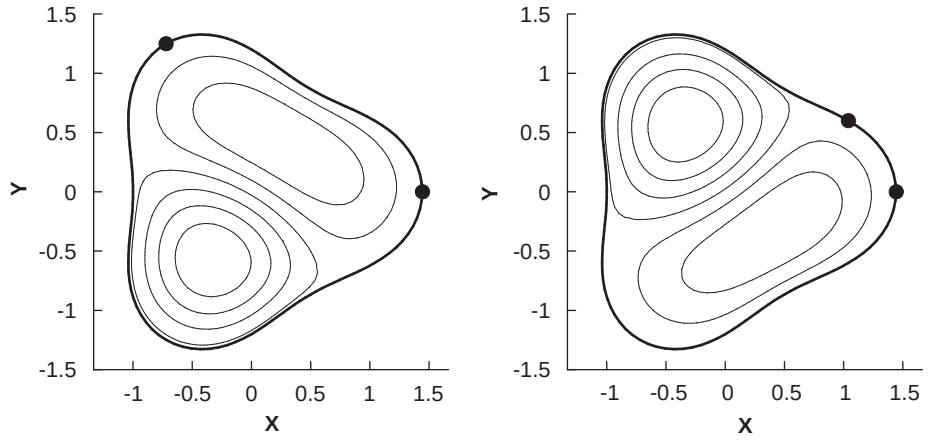

Fig. 21. Contours of the degenerate eigenmode after normalization obtained by the linear LSMFS (Example 3, modes 2, $b = 0.8$ and $N = 60$).

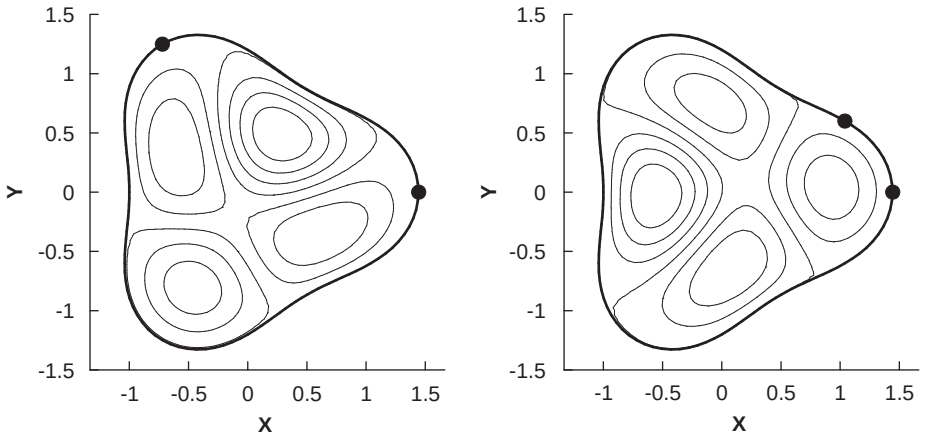

Fig. 22. Contours of the degenerate eigenmode after normalization obtained by the linear LSMFS (Example 3, modes 4, $b = 0.8$ and $N = 60$).

where

$$x = \rho \cos \theta$$
$$y = \rho \sin \theta$$

This problem does not have exact solution. Formally, the four lowest eigenvalues are obtained by the direct determinant search method (Fig. 16) as addressed, respectively, in Tables 7 and 8 for different nodes (N) and locations of source points (b). From Tables 7 and 8, it is very easy to observe rapid convergent behaviors of eigenvalues as b and N become larger. On the other hand, we also solve the same problem by the traditional FEM as stated in Table 9. In Table 9, the eigenvalues obtained by the FEM converge slowly when N become larger. Generally, the results of the linear LSMFS and FEM are in good agreement in the order of 10^{-3}–10^{-4}.

For the shapes of eigenmodes, we formally solve the problem by the linear LSMFS (Eq. (9)). The contours of the four lowest eigenmodes are depicted in Figs. 17–20, respectively. Here, we typically choose $b = 0.8$ and $N = 60$ based on the studies in Tables 7 and 8. The choice of these parameters is not an issue, since we have demonstrated in the previous examples that the shapes of eigenmodes are not sensitive with respect to b and N. For the first and third eigenmodes, they are not degenerate since the contours are almost the same in shape when the positions of specified normalized boundary data move (denoted by "●"). On the other hand, we can observe that the second and fourth eigenmodes are degenerate since the shapes of eigenmodes vary as the positions of specified normalized boundary data move. Therefore, we formally normalize the second and fourth eigenmodes by specifying two dual boundary data (Eq. (10)), as demonstrated, respectively, in Figs. 21 and 22, in which the results will ensure the degeneracy of these two eigenmodes. Based on these numerical results, it is convinced that the linear LSMFS is capable to determine the mode shapes of acoustical eigenmodes with and without degeneracy even for very complex problems without exact solutions.

4. Conclusions

A numerical scheme based on the linear LSMFS was proposed to obtain the mode shapes of acoustical eigenmodes with and without degeneracy for simple or complex domains. For nondegenerate modes, the eigenmodes are almost the same in shape except the specified normalized data at the boundary locations near or on the nodes ($\partial u/\partial n = 0$ for Dirichlet problems and $u = 0$ for Neumann problems). Moreover, the numerical results of mode shapes are generally insensitive to locations of source points. On the other hand, for the cases of degenerate modes, the mode shapes vary with respect to the locations of specified normalized boundary data. Thus, the normalized contours obtained by specifying two dual boundary data are demonstrated. Therefore, it is convinced that the linear LSMFS is a promising numerical method to obtain the

modal contours of acoustical eigenmodes robustly and is able to distinguish degenerate modes. Following the properties of the linear LSMFS, this method is free from meshes, singularities, as well as numerical integrations. Moreover, the robustness and accuracy of the eigenvalues obtained with respect to different locations of source points by the linear LSMFS in conjunction with direct determinant search method are also revisited.

Acknowledgments

The National Science Council of Taiwan is gratefully acknowledged for providing financial support to carry out the present work under the Grant no. NSC96-2221-E-464-001. We also like to thank the reviewers for very valuable comments to improve our paper.

References

[1] R.A. Gingold, J.J. Maraghan, Smoothed particle hydrodynamics: theory and applications to non-spherical stars, *Mon. Not. R. Astron. Soc.* 181 (1977) 375–389.
[2] V.D. Kupradze, M.A. Aleksidze, The method of functional equations for the approximate solution of certain boundary value problems, *USSR Comput. Math. Math. Phys.* 4 (4) (1964) 82–126.
[3] R. Mathon, R.L. Johnston, The approximate solution of elliptic boundary-value problems by fundamental solutions, *SIAM J. Numer. Anal.* 14 (1977) 638–650.
[4] A. Bogomolny, Fundamental solutions method for elliptic boundary value problems, *SIAM J. Numer. Anal.* 22 (1985) 644–669.
[5] R.L. Johnston, G. Fairweather, The method of fundamental solutions for problems in potential flow, *Appl. Math. Modelling* 8 (1984) 265–270.
[6] A. Karageorghis, G. Fairweather, The method of fundamental solutions for the numerical solution of the biharmonic equation, *J. Compu. Phys.* 69 (1987) 434–459.
[7] M.A. Golberg, The method of fundamental solutions for Poisson's equation, *Eng. Anal. Bound. Elem.* 16 (1995) 205–213.
[8] D.L. Young, S.J. Jane, C.M. Fan, K. Murugesan, C.C. Tsai, The method of fundamental solutions for 2D and 3D Stokes problems, *J. Compu. Phys.* 211 (2006) 1–8.
[9] D.L. Young, C.W. Chen, C.M. Fan, K. Murugesan, C.C. Tsai, Method of fundamental solutions for Stokes flows in a rectangular cavity with cylinders, *Euro. J. Mech. B: Fluid* 24 (2005) 703–716.
[10] D.L. Young, C.C. Tsai, K. Murugesan, C.M. Fan, C.W. Chen, Time-dependent fundamental solutions for homogeneous diffusion problems, *Eng. Anal. Bound. Elem.* 28 (2004) 1463–1473.
[11] D.L. Young, C.C. Tsai, C.M. Fan, Direct approach to solve nonhomogeneous diffusion problems using fundamental solutions and dual reciprocity methods, *J. Chin. Inst. Eng.* 27 (4) (2004) 597–609.
[12] M.A. Golberg, C.S. Chen, The method of fundamental solutions for potential, Helmholtz and diffusion problems, in: M.A. Golberg (Ed.), *Boundary Integral Methods: Numerical and Mathematical Aspects*, Computational Mechanics Publication, Southampton, Boston, 1998.
[13] G. Fairweather, A. Karageorghis, The method of fundamental solutions for elliptic boundary value problems, *Adv. Comput. Math.* 9 (1998) 69–95.
[14] G. Fairweather, A. Karageorghis, P.A. Martin, The method of fundamental solutions for scattering and radiation problems, *Eng. Anal. Bound. Elem.* 27 (2003) 759–769.
[15] J. Li, Y.C. Hon, C.S. Chen, Numerical comparisons of two meshless methods using radial basis function, *Eng. Anal. Bound. Elem.* 26 (2002) 205–225.
[16] P.S. Kondapalli, D.J. Shippy, G. Fairweather, Analysis of acoustic scattering in fluids and solids by the method of fundamental solutions, *J. Acoust. Soc. Am.* 91 (4) (1992) 1844–1854.
[17] A. Karageorghis, The method of fundamental solutions for the calculation of the eigenvalues of the Helmholtz equation, *Applied Math. Letters* 14 (2001) 837–842.
[18] J.T. Chen, I.L. Chen, Y.T. Lee, Eigensolutions of multiply connected membranes using the method of fundamental solutions, *Eng. Anal. Bound. Elem.* 29 (2005) 166–174.
[19] C.C. Tsai, D.L. Young, C.W. Chen, C.M. Fan, The method of fundamental solutions for eigenproblems in domains with and without interior holes, *Proc. R. Soc. A* 462 (2006) 1443–1466.
[20] S.Yu. Reutskiy, The method of fundamental solutions for Helmholtz eigenvalues problems in simply and multiply connected domains, *Eng. Anal. Bound. Elem.* 30 (2006) 150–159.
[21] C.J.S. Alves, S.S. Valtchev, Numerical comparison of two meshfree methods for acoustic wave scattering, *Eng. Anal. Bound. Elem.* 29 (2005) 371–382.
[22] S.W. Kang, J.M. Lee, Y.J. Kang, Vibration analysis of arbitrary shaped membranes using non-dimensional dynamic influence function, *J. Sound Vib.* 221 (1999) 117–132.
[23] S.W. Kang, J.M. Lee, Application of free vibration analysis of membranes using the non-dimensional dynamic influence function, *J. Sound Vib.* 234 (3) (2000) 455–470.

[24] S.W. Kang, J.M. Lee, Free vibration analysis of arbitrary shaped plates with clamped edges using wave-type function, *J. Sound Vib.* 242 (1) (2001) 9–26.
[25] J.T. Chen, S.R. Kuo, K.H. Chen, Y.C. Cheng, Comments on "Vibration analysis of arbitrary shaped membranes using non-dimensional dynamic influence function," *J. Sound Vib.* 235 (1) (2000) 156–171.
[26] W. Yeih, J.T. Chen, C.M. Chang, Applications of dual MRM for determining the natural frequencies and natural modes of an Euler–Bernoulli beam using the singular value decomposition method, *Eng. Anal. Bound. Elem.* 23 (1999) 339–360.
[27] J.T. Chen, C.X. Huang, F.C. Wong, Determination of spurious eigenvalues and multiplicities of true eigenvalues in the dual multiple reciprocity method using the singular-value decomposition technique, *J. Sound Vib.* 230 (2) (2000) 203–219.
[28] S.C. Lyngby, Condition number of matrices derived from two classes of integral equations, *Math. Meth. Applied Sci.* 3 (1981) 364–392.
[29] J.T. Chen, K.H. Chen, S.W. Chyuan, Numerical experiments for acoustic modes of a square cavity using the dual boundary element method, *Appl. Acoust.* 57 (1999) 293–325.
[30] Y.S. Smyrlis, A. Karageorghis, A linear least-squares MFS for certain elliptic problems, *Numer. Algor.* 35 (2004) 29–44.
[31] D.L. Young, C.M. Fan, C.C. Tsai, C.W. Chen, The method of fundamental solutions and domain decomposition method for degenerate seepage flownet problems, *J. Chin. Inst. Eng.* 29 (1) (2006) 63–73.